PERGAMON

International Journal of Solids and Structures 40 (2003) 3195–3210

INTERNATIONAL JOURNAL OF SOLIDS and STRUCTURES

www.elsevier.com/locate/ijsolstr

# Rapid sliding indentation with friction on a transversely isotropic thermoelastic half-space

L.M. Brock *

*Department of Mechanical Engineering, University of Kentucky, Lexington, KY 40506, USA*

Received 14 November 2002; received in revised form 27 January 2003

**Abstract**

A rigid insulated die slides at a constant sub-critical speed on a transversely isotropic half-space in the presence of friction. In a two-dimensional analysis of the dynamic steady-state, the coupled equations of thermoelasticity are invoked. All elements of the Coulomb friction model are strictly enforced, thus giving rise to auxiliary conditions, including two unilateral constraints.

Robust asymptotic forms of an exact solution to a related problem with unmixed boundary conditions lead to analytical solutions for the sliding indentation problem. The solution expressions, abetted by calculations for zinc, show the role of frictional heating on the half-space surface. The effects of friction and sliding speed on contact zone size and location and average contact zone temperature are also studied.

The analysis is aided by factoring procedures that simplify the complicated forms that arise in anisotropic elasticity. A scheme that renders expressions for roots of certain irrational functions analytic to within a single quadrature also plays a role.



*Keywords:* Anisotropy; Thermoelastic; Rapid sliding; Indentation; Frictional heating; Rayleigh speed

## 1. Introduction

Rapid sliding on elastic half-spaces by rigid dies provides a first step-model in studies of mechanisms and surface-finishing processes. Dynamic isothermal analyses of frictionless (Craggs and Roberts, 1967; Georgiadis and Barber, 1993) and friction-resisted (Brock, 1981) sliding exist, and Brock and Georgiadis (2000) have treated friction-resisted sliding as a coupled thermoelastic process in the dynamic steady-state. The half-spaces in these studies are isotropic. Brock et al. (2001) have considered the pure indentation of transversely isotropic or orthotropic half-spaces, and the sliding indentation case has been treated by Brock (2002). These two studies are isothermal and frictionless.

* Tel.: +1-859-257-2839; fax: +1-859-257-3304/8057.
*E-mail address:* brock@engr.uky.edu (L.M. Brock).


doi:10.1016/S0020-7683(03)00122-7

In this article, therefore, a two-dimensional steady-state dynamic analysis of sliding indentation on a transversely isotropic half-space governed by the equations of coupled thermoelasticity is performed. The die is insulated, is of infinite extent and constant cross-section in the direction perpendicular to sliding, and exhibits a smooth profile governed by Coulomb friction. The compressive force on the die and the sliding speed are treated as given. The latter is constant and sub-critical.

Physically acceptable solutions for sliding indentation allow the contact zone size and location to be determined for the given force and speed. Thus, the associated boundary value problem statement is augmented by auxiliary conditions. Of particular importance are the Signorini conditions (Georgiadis and Barber, 1993): (a) contact zone normal stress is non-tensile, and (b) indentor and half-space surfaces do not interpenetrate.

As is standard practice (Muskhelishvili, 1975) the Coulomb proportionality between normal and tangential resultant contact forces is guaranteed by enforcing the same proportionality between shear and (compressive) normal stress at every contact point. This gives a well-posed problem, but local enforcement of the Coulomb model also implies, in the strict sense, that the shear stress opposes at every contact point the relative motion (slip) of indentor and half-space. Therefore, this article imposes another unilateral constraint in addition to Signorini condition (a), that the contact zone shear stress everywhere exhibits a negative work-rate (Brock, 1981). To focus on physically relevant situations, the possibility of singular behavior, e.g. Brock (1981), is minimized by considering only continuous finite indentor profiles and profile slopes.

The general equations for transversely isotropic coupled thermoelasticity are presented in the next section, followed by statement of the sliding indentation problem in the dynamic steady-state. A simpler related problem is solved exactly in transform space, and robust asymptotics used for the transform inversions to reduce the sliding indentation study to a classical singular integral equation problem. Substantial use is made of Cauchy theory for integration—in particular, procedures used by Brock (1999) and Brock and Georgiadis (2000), hereafter denoted as BGB. Factoring procedures used by Brock et al. (2001) and Brock (2002), hereafter denoted as BGH, are also followed. These simplify the generally complicated forms that arise in anisotropic elasticity, e.g. Payton (1983) and Norris and Achenbach (1984). The solution process also requires, finally, the extraction of certain roots of irrational functions. In these instances, the approaches of Norris and Achenbach (1984) and Brock (1998), designated hereafter as NAB, are used.

## 2. General equations

Consider a homogeneous linearly thermoelastic half-space. It is defined in terms of the Cartesian coordinates $(x_1, x_2, x_3)$ as the region $x_2 > 0$ and is at rest at a uniform (absolute) temperature $T_0$. These coordinates also define the principal material axes of the half-space; the field equations for $x_2 > 0$ in the absence of body forces are then

$$\frac{\partial \sigma_{ik}}{\partial x_k} = \rho \ddot{u}_i, \quad K_i \frac{\partial^2 \theta}{\partial x_i^2} - T_0 \frac{\partial \sigma_{ik}}{\partial \theta} \dot{e}_{ik} - \rho c_v \dot{\theta} = 0 \tag{1a}$$

$$\sigma_{ik} = c_{ikjl} e_{jl} - \chi_i \theta \delta_{ik}, \quad 2e_{kl} = \frac{\partial u_k}{\partial x_l} + \frac{\partial u_l}{\partial x_k} \tag{1b}$$

Here $u_i$ is the displacement in the $x_i$-direction, and $\theta$ is the change in the temperature from the rest value $T_0$. All indices range over (1, 2, 3), $\delta_{ik}$ is the Kronecker delta, the summation convention holds, and $(\cdot)$ signifies time differentiation. The constants $(\rho, c_v, K_i)$ are the mass density, specific heat at constant strain, and thermal conductivity. The array $c_{ikjl}$ gives the isothermal elasticities. Symmetries allow contraction to the 21-member array $c_{mn} = c_{nm} (m, n = 1, 2, \ldots, 6)$ under the scheme in which subscript pairs $(ik)$ and $(jl)$ are replaced as follows: $(11) \to 1$, $(22) \to 2$, $(33) \to 3$, $(12) = (21) \to 4$, $(23) = (32) \to 5$, $(31) = (13) \to 6$. In this format the term

$$\chi_i = c_{ik}\alpha_k \quad (i, k = 1, 2, 3) \tag{2}$$

where $\alpha_k$ are coefficients of thermal expansion. For the transversely isotropic case here, the $x_2$-axis is one of material symmetry, and

$$K_3 = K_1, \quad \alpha_3 = \alpha_1 \tag{3a}$$

$$c_{33} = c_{11}, \quad c_{55} = c_{44}, \quad 2c_{66} = c_{11} - c_{13}, \quad c_{23} = c_{12} \tag{3b}$$

$$c_{ik} = 0 \ (i = 1, 2, 3; k = 4, 5, 6), \quad c_{45} = c_{56} = 0 \tag{3c}$$

subject to the restrictions

$$(K_1, K_2) > 0, \quad (\alpha_1, \alpha_2) > 0, \quad c_v > 0 \tag{4a}$$

$$c_{11} > |c_{13}|, \quad (c_{11} + c_{13})c_{22} > 2c_{12}^2, \quad c_{44} > 0 \tag{4b}$$

The inequalities (4a) are based on thermodynamic considerations (Boley and Wiener, 1985) while (4b) guarantees that the array $c_{ikjl}$ gives a positive-definite fourth-order tensor (Payton, 1983).

## 3. Sliding indentation problem

A plane-strain state is induced in this half-space by an insulated rigid die of uniform cross-section and infinite extent in the $x_3$-direction. It is simultaneously translated in the positive $x_1$-direction with constant sub-critical speed $v$ and pressed into the half-space surface with force (per unit length in the $x_3$-direction) $F$. This process is resisted by Coulomb friction, and eventually attains a dynamic steady-state. It is, therefore, convenient to translate coordinates in the sliding direction with the same speed. Then, as depicted schematically in Fig. 1, $(x_2 = 0, x_1 = L_\pm)$ always locate the contact zone edges, where $L = L_+ - L_- > 0$ is the zone size. The lengths $(L, L_\pm)$ are a priori unknown. The plane-strain nature of the process implies that $(u_1, u_2, \theta)$ and the stresses $(\sigma_{11}, \sigma_{22}, \sigma_{12}, \sigma_{33})$ are the non-trivial dependent variables. The steady-state nature implies that these depend only on $(x_1, x_2)$, and that time derivatives in the moving coordinates can be neglected, i.e. $(\cdot) = -v\partial(\ )/\partial x_1$. It is also convenient to introduce the parameters

$$v_r^0 = \sqrt{\frac{c_{44}}{\rho}}, \quad h = \frac{K_1 + K_2}{2v_r^0 c_v \rho}, \quad \varepsilon_k = \frac{T_0}{c_v}(v_r^0 \tilde{\alpha} \Gamma_k)^2 \quad (k = 1, 2) \tag{5a}$$

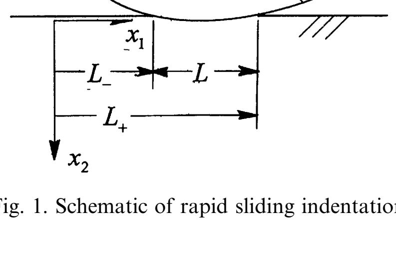


Fig. 1. Schematic of rapid sliding indentation.

$$\tilde{\alpha}\Gamma_1 = (\beta + m_3 - 1)\alpha_1 + (m - 1)\alpha_2, \quad \tilde{\alpha}\Gamma_2 = 2(m - 1)\alpha_1 + \alpha\alpha_2 \tag{5b}$$

$$\tilde{\alpha} = \frac{1}{3}(2\alpha_1 + \alpha_2) \tag{5c}$$

where $(v_r^0, \tilde{\alpha})$ are the shear wave speed in an isotropic solid with shear modulus $c_{44}$ and average thermal expansion and, after Payton (1983), the dimensionless quantities

$$\alpha = \frac{c_{22}}{c_{44}}, \quad \beta = \frac{c_{11}}{c_{44}}, \quad m = 1 + \frac{c_{12}}{c_{44}}, \quad m_3 = 1 + \frac{c_{13}}{c_{44}}, \quad \gamma = 1 + \alpha\beta - m^2 \tag{6}$$

In view of (6) $h$ is a thermoelastic characteristic length, $(\varepsilon_1, \varepsilon_2)$ are dimensionless thermoelastic coupling constants, and the dimensionless quantities $(\Gamma_1, \Gamma_2)$ both characterize these constants and influence the solution in their own right. The characteristic length suggests that the dimensionless variables $(\xi, \eta, c, k_i)$ be introduced:

$$(x_1, x_2) = (h\xi, h\eta), \quad v = cv_r^0, \quad k_i = \frac{2K_i}{K_1 + K_2}(i = 1, 2) \tag{7}$$

In view of (2) and (5)–(7) the general field equations (1) give the pertinent forms

$$(\beta - c^2)u_{1,\xi\xi} + u_{1,\eta\eta} + mu_{2,\xi\eta} - h\tilde{\alpha}\Gamma_1\theta_{,\xi} = 0 \tag{8a}$$

$$mu_{1,\xi\eta} + (1 - c^2)u_{2,\xi\xi} + \alpha u_{2,\eta\eta} - h\tilde{\alpha}\Gamma_2\theta_{,\eta} = 0 \tag{8b}$$

$$h(k_1\theta_{,\xi\xi} + k_2\theta_{,\eta\eta}) + c\left[h\theta + \frac{1}{\tilde{\alpha}}\left(\Gamma_1 u_{1,\xi} + \Gamma_2 u_{2,\eta}\right)\right]_{,\xi} = 0 \tag{8c}$$

for $\eta > 0$, subject to the constitutive relations

$$\frac{h}{c_{44}}\sigma_{11} = \beta u_{1,\xi} + (m - 1)u_{2,\eta} - h\tilde{\alpha}\Gamma_1\theta \tag{9a}$$

$$\frac{h}{c_{44}}\sigma_{22} = (m - 1)u_{1,\xi} + \alpha u_{2,\eta} - h\tilde{\alpha}\Gamma_2\theta \tag{9b}$$

$$\frac{h}{c_{44}}\sigma_{12} = u_{1,\eta} + u_{2,\xi} \tag{9c}$$

where $(\ )_{,x} = \partial(\ )/\partial x$. In light of (7) the boundary conditions for $\eta = 0$ become

$$(\sigma_{12}, \sigma_{22}) = 0(\xi \notin L); \quad \sigma_{12} = \mu\sigma_{22}, \quad u_{2,\xi} = \frac{\mathrm{d}V(\xi)}{\mathrm{d}\xi}(\xi \in L); \quad \theta_{,\eta} = 0 \tag{10}$$

Eq. (7) gives rise to dimensionless contact zone parameters $(l_\pm, l)$ defined by

$$(L_+, L_-) = (hl_+, hl_-), \quad L = hl \tag{11}$$

The dimensionless quantity $\mu$ is the sliding (kinetic) friction coefficient, and the last condition in (10)—which holds for all $\eta = 0$—represents die insulation. Experimental data, e.g. (Blau, 1996), suggests that $0 < \mu < 1$ for most material combinations, especially metal/metal. Although the present analysis can treat values in excess of unity, the limitation $0 < \mu < 1$ is observed in calculations. It is noted that the symbol $L$ is also used to represent the contact zone itself. The function $V(\xi)$ is the normal displacement imposed by the die profile in the contact zone, and $(V, \mathrm{d}V/\mathrm{d}\xi)$ must be finite and continuous. The condition involving $\mathrm{d}V/\mathrm{d}\xi$, in (10) is sufficient to obtain a steady-state solution to within a rigid body translation. The restrictions on $V$ imply that $(u_1, u_2, \theta)$ should be finite and continuous almost everywhere.

For the solution to this mixed boundary value problem to be physically acceptable, first of all, the total (compressive) force (per unit length in the $x_3$-direction) on the contact zone must be the given $F$:

$$h\int_L \sigma_{22}\,\mathrm{d}\xi = -F \tag{12}$$

The symbol $L$ also signifies that integration is over the range $(l_-, l_+)$. Then, Signorini conditions must be satisfied: After Georgiadis and Barber (1993) and Brock and Georgiadis (2000), these consist of two parts. Condition (a) requires that

$$\sigma_{22} \leqslant 0 \quad (\eta = 0, \xi \in L) \tag{13}$$

Condition (b) requires in effect that stresses are at least finite at the contact zone edges ($\xi = l_\pm$). Finally, a local negative shear work rate requires, in its steady-state form, that

$$\sigma_{12} v(h + u_{1,\xi}) < 0 \quad (\eta = 0, \xi \in L) \tag{14}$$

In light of (10) and (13), this reduces to the local unilateral constraint

$$u_{1,\xi} \geqslant -h \quad (\eta = 0, \xi \in L) \tag{15}$$

In view of (7), violation of this constraint requires a displacement gradient on the order of unity. It will be seen that such a state can be approached theoretically as the sliding speed tends to a critical value.

## 4. Unmixed problem: transform solution

Consider now a related problem that satisfies (8) and (9) and the unmixed conditions

$$\sigma_{22} = \sigma(\xi), \quad \sigma_{12} = \mu\sigma(\xi), \quad \theta_{,\eta} = 0 \tag{16a}$$

$$\sigma(\xi) = 0 \quad (\xi \notin L) \tag{16b}$$

on $\eta = 0$. Here $\sigma(\xi)$ is a largely arbitrary function, continuous and finite for $\xi \in L$. This unmixed problem gives a candidate for the solution to the sliding indentation problem if $\sigma(\xi)$ is interpreted as the contact zone normal stress and satisfies the condition on $u_{2,\xi}$ in (10). The candidate becomes the solution itself if the unilateral constraint (13) and (15), and Signorini condition (b) are also satisfied.

To solve the system (8), (9) and (16) the bilateral Laplace transform (van der Pol and Bremmer, 1950) and its inverse, respectively, are introduced as

$$\hat{f} = \int_{-\infty}^{\infty} f(\xi)\mathrm{e}^{-p\xi}\,\mathrm{d}\xi, \quad f(\xi) = \frac{1}{2\pi i}\int \hat{f}\mathrm{e}^{p\xi}\,\mathrm{d}p \tag{17}$$

In the first integral $p$ is imaginary, while the second integration is along the Bromwich contour in the complex $p$-plane. Application of the transform operation to (8) and (9) gives for $\eta > 0$ the pertinent transform sets

$$\hat{u}_1 = \frac{\tilde{\alpha}}{p}\sum Q_i U_i \mathrm{e}^{-pq_i\eta}, \quad \hat{u}_2 = -\tilde{\alpha}\sum q_i Q_i V_i \mathrm{e}^{-pq_i\eta}, \quad h\hat{\theta} = \sum Q_i \mathrm{e}^{-pq_i\eta} \tag{18}$$

$$\frac{h}{c_{44}}\hat{\sigma}_{22} = \tilde{\alpha}\sum Q_i[(m-1)U_i + \alpha q_i^2 V_i - \Gamma_2]\mathrm{e}^{-pq_i\eta} \tag{19a}$$

$$\frac{h}{c_{44}}\hat{\sigma}_{12} = -\tilde{\alpha}p\sum Q_i(U_i + V_i)\mathrm{e}^{-pq_i\eta} \tag{19b}$$

$$h\hat{\theta}_{,\eta} = -p^2 \sum q_i Q_i \mathrm{e}^{-pq_i\eta} \tag{19c}$$

where $\sum$ implies summation over the range $i = (1, 2, 3)$. In (18) and (19) the $Q_i$ are unknown functions of $(p, q_i)$, and the dimensionless quantities

$$g(q_i)U_i = B^2\Gamma_1 + (\alpha\Gamma_1 - m\Gamma_2)q_i^2, \quad g(q_i)V_i = \alpha A^2\Gamma_2 + (q_i^2 - m)\Gamma_1 \tag{20a}$$

$$g(q) = (\alpha A^2 + q^2)(B^2 + \alpha q^2) - m^2 q^2 \tag{20b}$$

$$\sqrt{\alpha}A = \sqrt{\beta - c^2}, \quad B = \sqrt{1 - c^2} \tag{20c}$$

Here $(q_1^2, q_2^2, q_3^2)$ are the roots of the cubic

$$\left(k_1 + k_2 q^2 + \frac{c}{p}\right)g(q) + \frac{c}{p}\left[\varepsilon_1(B^2 + \alpha q^2) + \varepsilon_2 q^2(\alpha A^2 + q^2) - 2m\sqrt{\varepsilon_1\varepsilon_2}q^2\right] \tag{21}$$

These roots need not be single-valued in $p$ but, in order that (18) and (19) be bounded as $\eta \to \infty$, must give $\mathrm{Re}(pq_i) \geqslant 0$ in the cut $p$-plane. The $Q_i$ follow by substituting (19) into the transform of (16a):

$$Q_i = \frac{h}{\tilde{\alpha}c_{44}} \frac{g(q_i)}{\Delta}(q_j - q_k)\left[\alpha H(q_j, q_k)\mu\hat{\sigma} + q_j q_k(q_j + q_k)G(q_j^2, q_k^2)\hat{\sigma}\right] \tag{22a}$$

$$\Delta = \sum_{i=1}^{3} (N_\Gamma q_i^2 + M_\Gamma B^2)q_j q_k\left(q_j^2 - q_k^2\right)G\left(q_j^2, q_k^2\right) \tag{22b}$$

$$\hat{\sigma} = \int_L \sigma(t)\mathrm{e}^{-pt}\,\mathrm{d}t \tag{22c}$$

In (22a,b) $i \neq j \neq k$ and the three indices cycle through the values (1,2,3), e.g. $(i = 1, j = 2, k = 3)$. The dimensionless terms $(G, H)$ are given by

$$G(x^2, y^2) = K_\Gamma(x^2 + y^2) + L_\Gamma x^2y^2 + K_\Gamma T - L_\Gamma A^2B^2 \tag{23a}$$

$$\begin{aligned} H(x, y) = {} & M_\Gamma A^2B^4 + [N_\Gamma(x^2y^2 - A^2B^2) + M_\Gamma(T + x^2 + y^2)]xy + M_\Gamma B^2(x^2 + y^2)^2 \\ & + (M_\Gamma B^2T + N_\Gamma x^2y^2)(x^2 + y^2) + (N_\Gamma T - M_\Gamma B^2)x^2y^2 \end{aligned} \tag{23b}$$

and the dimensionless parameters

$$T = \alpha A^2 + \frac{1}{\alpha}(B^2 - m^2) \tag{24a}$$

$$K_\Gamma = (B^2 - m)\Gamma_1 + \alpha A^2\Gamma_2, \quad L_\Gamma = \alpha\Gamma_1 + (1 - m)\Gamma_2 \tag{24b}$$

$$M_\Gamma = (m - 1)\Gamma_1 - \alpha A^2\Gamma_2, \quad N_\Gamma = -\alpha\Gamma_1 + (m - B^2)\Gamma_2 \tag{24c}$$

depend only on dimensionless thermoelastic constants and the dimensionless sliding speed $c$. With (18), (19) and (22) available, the solution to the unmixed problem in transform space is essentially complete. However, the roots $q_i^2$ exhibit a type of $p$-dependence that leads, upon transform inversion, to multiple integrals of $\sigma$. While not complicated, their presence could require that the boundary condition on $u_{2,\xi}$ in (10) be solved for $\sigma$ by semi-numerical techniques. Asymptotic forms of (18), (19) and (22) are, therefore, sought that allow an analytical solution.

## 5. Unmixed problem: asymptotic solution

Asymptotic forms of the bilateral Laplace transform valid for $|p| \ll 1$ give inversions that are valid for $|\xi| \gg 1$. However, because $h$ is usually (Brock and Georgiadis, 2000) of an order of magnitude less than 1 μm, the inversions are robust. Therefore (18) and (19) are expanded in view of (20), (22a,b) and (23) for small $|p|$, and only the lowest-order terms kept. In particular, the roots of (21) give

$$q_1 = a\hat{\partial}, \quad q_2 = b\hat{\partial}, \quad \sqrt{p}q_3 = \sqrt{c_\varepsilon}\hat{\partial}, \quad \hat{\partial} = \frac{\sqrt{-p}}{\sqrt{p}} \tag{25}$$

where the dimensionless quantities $(a, b, c_\varepsilon)$ are defined by (5) and

$$a = \Omega + \omega, \quad b = \Omega - \omega, \quad c_\varepsilon = \frac{c}{k_2}\frac{\alpha_\varepsilon}{\alpha} \tag{26a}$$

$$2\sqrt{\alpha_\varepsilon}(\Omega, \omega) = \sqrt{(\alpha_\varepsilon A_\varepsilon \pm B)^2 - m_\varepsilon^2}, \quad \sqrt{\alpha_\varepsilon}A_\varepsilon = \sqrt{\beta_\varepsilon - c^2}, \quad ab = A_\varepsilon B \tag{26b}$$

$$\alpha_\varepsilon = \alpha + \varepsilon_2, \quad \beta_\varepsilon = \beta + \varepsilon_1, \quad m_\varepsilon = m + \sqrt{\varepsilon_1\varepsilon_2}, \quad \gamma_\varepsilon = 1 + \alpha_\varepsilon\beta_\varepsilon - m_\varepsilon^2 \tag{26c}$$

The transforms (18) become, for example,

$$\frac{c_{44}}{h}\hat{u}_1 = \frac{U_a e^{-a\eta\sqrt{-p}\sqrt{p}}}{B(b-a)R_\varepsilon D}(K_b b\hat{\sigma} + N_b\hat{\partial}\mu\hat{\sigma}) - \frac{U_b e^{-b\eta\sqrt{-p}\sqrt{p}}}{B(b-a)R_\varepsilon D}(K_a a\hat{\sigma} + N_a\hat{\partial}\mu\hat{\sigma}) \tag{27a}$$

$$\frac{c_{44}}{h}\hat{u}_2 = \frac{aV_a e^{-a\eta\sqrt{-p}\sqrt{p}}}{B(b-a)R_\varepsilon D}(N_b\mu\hat{\sigma} - K_b b\hat{\partial}\hat{\sigma}) - \frac{bV_b e^{-b\eta\sqrt{-p}\sqrt{p}}}{B(b-a)R_\varepsilon D}(N_a\mu\hat{\sigma} - K_a a\hat{\partial}\hat{\sigma}) \tag{27b}$$

$$c_{44}\tilde{\alpha}\hat{\theta} = \frac{\alpha\Theta_a a e^{-a\eta\sqrt{-p}\sqrt{p}}}{B(b-a)R_\varepsilon D}(K_b b\hat{\sigma} + N_b\hat{\partial}\mu\hat{\sigma}) - \frac{\alpha\Theta_b b e^{-b\eta\sqrt{-p}\sqrt{p}}}{B(b-a)R_\varepsilon D}(K_a a\hat{\sigma} + N_a\hat{\partial}\mu\hat{\sigma}) \tag{27c}$$

Here (19) and (20) produce in light of (25) the dimensionless terms

$$(U_a, U_b) = B^2\Gamma_1 + (m\Gamma_2 - \alpha\Gamma_1)(a^2, b^2) \tag{28a}$$

$$(V_a, V_b) = \alpha A^2\Gamma_2 - m\Gamma_1 - \Gamma_1(a^2, b^2) \tag{28b}$$

$$(K_a, K_b) = K_\Gamma - L_\Gamma(a^2, b^2), \quad (N_a, N_b) = N_\Gamma(a^2, b^2) - M_\Gamma B^2 \tag{28c}$$

$$\Theta_a = a^4 - Ta^2 + A^2B^2, \quad \Theta_b = b^4 - Tb^2 + A^2B^2 \tag{28d}$$

and dimensionless parameters

$$R_\varepsilon = c^2A_\varepsilon + C_R B, \quad T_\varepsilon = \alpha_\varepsilon A_\varepsilon^2 + \frac{1}{\alpha_\varepsilon}(B^2 - m_\varepsilon^2) \tag{29a}$$

$$DC_R = M_\Gamma(K_\Gamma - L_\Gamma T_\varepsilon) + L_\Gamma N_\Gamma A_\varepsilon^2, \quad c^2D = K_\Gamma N_\Gamma - L_\Gamma M_\Gamma B^2 \tag{29b}$$

## 6. Sliding speed and material effects

If $\mathrm{Re}(a, b) \geqslant 0$, then boundedness of (27) as $\eta \to \infty$ is assured if the branch cuts $\mathrm{Im}(p) = 0$, $\mathrm{Re}(p) < 0$ and $\mathrm{Im}(p) = 0$, $\mathrm{Re}(p) > 0$ are introduced for $\sqrt{\pm p}$ respectively, and $\mathrm{Re}(\sqrt{\pm p}) \geqslant 0$ in the cut $p$-plane. Study of (20c) and (26a,b) shows that $c = \pm(1, \sqrt{\beta}, \sqrt{\beta_\varepsilon})$ are branch points of $(B, b), A$ and $(A_\varepsilon, a)$, respectively, in the $c$-plane. We impose, therefore, the requirements that $\mathrm{Re}(B, b, A, A_\varepsilon, a) \geqslant 0$ in the cut $c$-plane. In light of (5a) and (7), the general property $\beta > 1$ (Payton, 1983) implies that $(\sqrt{\beta} v_r^0, v_r^0)$ are, respectively, the isothermal dilatational and rotational wave speeds parallel to the $x_1$-axis, while $(\sqrt{\beta_\varepsilon} v_r^0, v_r^0)$ are (asymptotically) their thermoelastic counterparts. Therefore, limiting the present study to sub-critical sliding speeds requires as a first step that $0 < c < 1$, i.e. $(B, A, A_\varepsilon)$ in (27) are always positive real.

The terms $(a, b)$ exhibit branch points in addition to the values $c = \pm(1, \sqrt{\beta_\varepsilon})$ shared with $(B, A_\varepsilon)$. By generalizing the isothermal transversely isotropic results of Payton (1983), three categories for the dimensionless thermoelastic parameters $(\alpha_\varepsilon, \beta_\varepsilon, \gamma_\varepsilon)$ can be defined according to the locations of these additional branch points:

$$\begin{aligned} &\text{Category 1}: 2\sqrt{\alpha_\varepsilon \beta_\varepsilon} \leqslant \gamma_\varepsilon \leqslant 1 + \alpha_\varepsilon \beta_\varepsilon \quad (1 < \beta_\varepsilon < \alpha_\varepsilon) \\ &\alpha_\varepsilon + \beta_\varepsilon \leqslant \gamma_\varepsilon \leqslant 1 + \alpha_\varepsilon \beta_\varepsilon \quad (1 < \alpha_\varepsilon < \beta_\varepsilon) \\ &2\alpha_\varepsilon \leqslant \gamma_\varepsilon \leqslant 1 + \alpha_\varepsilon^2 \quad (1 < \beta_\varepsilon = \alpha_\varepsilon) \end{aligned} \tag{30a}$$

$$\text{Category 2}: 1 + \beta_\varepsilon < \gamma_\varepsilon < \alpha_\varepsilon + \beta_\varepsilon, \quad \gamma_\varepsilon^2 - 4\alpha_\varepsilon \beta_\varepsilon < 0 \tag{30b}$$

$$\text{Category 3}: \gamma_\varepsilon < 1 + \beta_\varepsilon, \quad \gamma_\varepsilon^2 - 4\alpha_\varepsilon \beta_\varepsilon < 0 \tag{30c}$$

The associated cuts are chosen so that the property $\mathrm{Re}(a, b) \geqslant 0$ is maintained in the cut $c$-plane. In this article, however, it is useful to seek the branch points of the combinations $b \pm a$. For category 3, the terms $b \pm a$ exhibit, respectively, the branch points

$$c = \pm c', \quad c' = \sqrt{1 - \frac{1}{(\alpha_\varepsilon - 1)^2}\left[\sqrt{\alpha_\varepsilon}\sqrt{m_\varepsilon^2 - (\alpha_\varepsilon - 1)(\beta_\varepsilon - 1)} - m_\varepsilon\right]^2} \tag{31a}$$

$$c = \pm \mathrm{i}c'', \quad c'' = \sqrt{\frac{1}{(\alpha_\varepsilon - 1)^2}\left[\sqrt{\alpha_\varepsilon}\sqrt{m_\varepsilon^2 - (\alpha_\varepsilon - 1)(\beta_\varepsilon - 1)} + m_\varepsilon\right]^2 - 1} \tag{31b}$$

For category 1 and 2, the term $b - a$ has, respectively, the branch points

$$c = \pm c_c, \quad c_c = \sqrt{\frac{1}{(\alpha_\varepsilon - 1)^2}\left[m_\varepsilon \pm \mathrm{i}\sqrt{\alpha_\varepsilon}\sqrt{(\alpha_\varepsilon - 1)(\beta_\varepsilon - 1) - m_\varepsilon^2}\right]^2 - 1} \tag{32a}$$

$$c = \pm \mathrm{i}c'' \tag{32b}$$

Eqs. (31) and (32) show that the categories coalesce to some extent in so far as the branch points of the linear combinations of $(a, b)$ are concerned. It should also be noted that, after BGH, the denominator term $b - a$ has been factored from the original solution forms. The potential singular behavior does not, as seen in (31) and (32), arise for real sliding speeds. In fact, such behavior would not occur in any case: the exponential terms in (27) are identical when $b = a$, and combinations of the now-common numerator terms themselves exhibit factors $b - a$ that cancel that in the denominator.

However, $0 < c' < 1$ in (31a). Thus, the quantities $(a, b, a + b)$ are given by (26a) and are positive real on the positive $\mathrm{Re}(c)$-axis for $0 < c < 1$ for all subsonic sliding speeds $(0 < v < v_r^0)$ in the category 1 and 2 case, but only for $c' < c < 1$ when subsonic speeds lie in the range $c' v_r^0 < v < v_r^0$ in the category 3 case. For speeds in the subsonic range $0 < v < c' v_r^0$ the combination $b + a$ remains positive real for category 3 in the interval $0 < c < c'$ of the positive $\mathrm{Re}(c)$-axis, but $(a, b)$ are now the complex conjugates

$$a = \Omega \mp \mathrm{i}\bar{\omega}, \quad b = \Omega \pm \mathrm{i}\bar{\omega} \tag{33}$$

for $\text{Im}(c) = 0\pm, 0 < c < c'$, where

$$2\sqrt{\alpha_\varepsilon}\bar{\omega} = \sqrt{m_\varepsilon^2 - (\alpha_\varepsilon A_\varepsilon - B)^2} \tag{34}$$

Eq. (27) is bounded in $\eta$ for all subsonic speeds because $\Omega > (\omega, \bar{\omega}) > 0$. Moreover, the real-valued nature of $c$-dependence in (27) is maintained even when $0 < c < c'$ because the pairs of terms in (27) become complex conjugates in view of (33).

Another denominator term in (27), $R_\varepsilon$, is also obtained by factoring the original forms after BGH. It is a more compact version of the thermoelastic Rayleigh function of the speed parameter $c$, where

$$R_\varepsilon(0) < 0, \quad R_\varepsilon(\pm 1) > 0, \quad R_\varepsilon(\pm c_R^\varepsilon) = 0 \quad (0 < c_R^\varepsilon < 1) \tag{35}$$

That is, $c_R^\varepsilon v_R^0$ is the effective thermoelastic Rayleigh speed parallel to the $x_1$-axis. By following NAB, the dimensionless Rayleigh speed parameter can be obtained analytically to within a single quadrature as

$$c_R^\varepsilon = \frac{1}{G_R}\sqrt{\frac{-\sqrt{\alpha_\varepsilon}R_0}{\sqrt{\beta_\varepsilon}(1+\sqrt{\alpha_\varepsilon})}}, \quad \ln G_R = -\frac{1}{\pi}\int_1^{\sqrt{\beta_\varepsilon}} \tan^{-1}\frac{C_R\sqrt{\alpha_\varepsilon}}{t^2}\sqrt{\frac{t^2-1}{\beta_\varepsilon - t^2}}\frac{\mathrm{d}t}{t} \tag{36}$$

In (36) the definitions

$$R_0 = \frac{-1}{K_0\Gamma_2 + L_0\Gamma_1 - K_0L_0}\left[(K_0 - L_0\beta_\varepsilon)\left(K_0 - \frac{L_0}{\alpha_\varepsilon}\right) + K_0L_0\frac{m_\varepsilon^2}{\alpha_\varepsilon}\right] < 0 \tag{37a}$$

$$K_0 = (1-m)\Gamma_1 + \beta\Gamma_2, \quad L_0 = \alpha\Gamma_1 + (1-m)\Gamma_2 \tag{37b}$$

hold. Because (27) is singular at $c = \pm c_R^\varepsilon$ we define sub-critical sliding indentation speed as being that for which

$$0 < c < c_R^\varepsilon \tag{38}$$

## 7. Unmixed problem: full-field solution example

For (27) governed by either (26a) or (33), the entire $\text{Im}(p)$-axis serves as the Bromwich contour in (17). Integration along this axis is accomplished with standard tables (Peirce and Foster, 1956). Eq. (27a) then gives

$$\begin{aligned}\frac{c_{44}}{h}u_{1,\xi} = {} & \frac{-1}{2\pi R_\varepsilon}(C_LB + A_\varepsilon)\int_L \sigma\left(\frac{\Omega\eta}{\tau_+^2 + \Omega^2\eta^2} + \frac{\Omega\eta}{\tau_-^2 + \Omega^2\eta^2}\right)\mathrm{d}t \\ & + \frac{\Omega}{2\pi\bar{\omega}R_\varepsilon}(C_LB - A_\varepsilon)\int_L \sigma\left(\frac{\tau_+}{\tau_+^2 + \Omega^2\eta^2} - \frac{\tau_-}{\tau_-^2 + \Omega^2\eta^2}\right)\mathrm{d}t \\ & + \frac{\mu B}{2\pi\bar{\omega}R_\varepsilon}\left(C_N - \frac{T_\varepsilon}{2}\right)\int_L \sigma\left(\frac{\Omega\eta}{\tau_+^2 + \Omega^2\eta^2} - \frac{\Omega\eta}{\tau_-^2 + \Omega^2\eta^2}\right)\mathrm{d}t \\ & - \frac{\mu B\Omega}{\pi R_\varepsilon}\int_L \sigma\left(\frac{\tau_+}{\tau_+^2 + \Omega^2\eta^2} + \frac{\tau_-}{\tau_-^2 + \Omega^2\eta^2}\right)\mathrm{d}t\end{aligned} \tag{39}$$

for category 3 when $0 < c < c'$, where $\sigma(t)$ is understood and

$$\tau_\pm = \tau \pm \bar{\omega}\eta, \quad \tau = \xi - t \tag{40a}$$

$$DC_L = \Gamma_1(T_\varepsilon L_\Gamma - K_\Gamma) + L_\Gamma A_\varepsilon^2(\alpha\Gamma_1 - m\Gamma_2) \tag{40b}$$

$$DC_N = \Gamma_1(T_\varepsilon N_\Gamma - M_\Gamma B^2) + N_\Gamma A_\varepsilon^2(m\Gamma_2 - \alpha\Gamma_1) \tag{40c}$$

For category 1 and 2 for all $0 < c < 1$ and category 3 when $c' < c < 1$, however,

$$\begin{aligned}\frac{c_{44}}{h}u_{1,\xi} = {} & \frac{-1}{2\pi R_\varepsilon}(C_L B + A_\varepsilon)\int_L \sigma\left(\frac{b\eta}{\tau^2 + b^2\eta^2} + \frac{a\eta}{\tau^2 + a^2\eta^2}\right)\mathrm{d}t + \frac{\Omega}{2\pi\omega R_\varepsilon}(C_L B - A_\varepsilon) \\ & \times \int_L \sigma\left(\frac{b\eta}{\tau^2 + b^2\eta^2} - \frac{a\eta}{\tau^2 + a^2\eta^2}\right)\mathrm{d}t + \frac{\mu B}{2\pi\omega R_\varepsilon}\left(C_N - \frac{T_\varepsilon}{2}\right)\int_L \sigma\left(\frac{\tau}{\tau^2 + b^2\eta^2} - \frac{\tau}{\tau^2 + a^2\eta^2}\right)\mathrm{d}t \\ & - \frac{\mu B\Omega}{\pi R_\varepsilon}\int_L \sigma\left(\frac{\tau}{\tau^2 + b^2\eta^2} + \frac{\tau}{\tau^2 + a^2\eta^2}\right)\mathrm{d}t\end{aligned} \tag{41}$$

Similar results hold for $(u_{2,\xi}, \theta)$. Eqs. (39) and (41) coincide in the limit as $c \to c'$ and as $\eta \to 0$.

## 8. Sliding indentation problem solution

The simpler problem results provide a candidate for the sliding indentation problem solution if the condition on $u_{2,\xi}$ in (10) is satisfied. Substitution of the counterpart to (39) and (41) into this condition and invoking the standard (Carrier and Pearson, 1988) result

$$\frac{x}{x^2 + y^2} \to \pi\delta(y) \quad (x \to 0+) \tag{42}$$

where $\delta$ is the Dirac function, leads to the equation

$$2\Omega A_\varepsilon \frac{1}{\pi}(P)\int_L \frac{\sigma \mathrm{d}t}{t - \xi} + (A_\varepsilon + C_M B)\mu\sigma = \frac{c_{44}R_\varepsilon}{h}\frac{\mathrm{d}V}{\mathrm{d}\xi} \quad (\xi \in L) \tag{43}$$

for $\sigma$. Here $(P)$ signifies Cauchy principal value integration, and the dimensionless quantity $C_M$ is given by

$$DC_M = \Gamma_2(N_\Gamma A_\varepsilon^2 - M_\Gamma) + M_\Gamma(\alpha A^2\Gamma_2 - m\Gamma_1) \tag{44}$$

Eq. (43) is a standard (Muskhelishvili, 1975; Erdogan, 1976) singular integral equation; in the manner of BGB it yields the solution

$$\frac{\sigma}{c_{44}} = \frac{R_\varepsilon}{hA_\varepsilon D_\Omega}\Im\left(\frac{\mathrm{d}V}{\mathrm{d}\xi};\xi\right), \quad D_\Omega = \sqrt{4\Omega^2 + \mu^2\left(1 + C_M\frac{B}{A_\varepsilon}\right)^2} \tag{45}$$

where the functional

$$\Im(X;x) = X(x)\cos\pi\upsilon + \left(\frac{l_+ - x}{x - l_-}\right)^\upsilon \frac{\sin\pi\upsilon}{\pi}(P)\int_L \frac{X(t)}{t - x}\left(\frac{t - l_-}{l_+ - t}\right)^\upsilon \mathrm{d}t \quad (x \in L) \tag{46a}$$

$$\upsilon = \frac{1}{\pi}\tan^{-1}\frac{\mu}{2\Omega}\left(1 + C_M\frac{B}{A_\varepsilon}\right) - \frac{1}{2}\left(-\frac{1}{2} < \upsilon < 0\right) \tag{46b}$$

Eq. (46b) gives the eigenvalue of (43). Its sign indicates in light of (16a) that the solution candidate (45) automatically satisfies Signorini condition (b) at $\xi = l_-$.

Satisfaction at $\xi = l_+$, however, requires that

$$\int_L \frac{\mathrm{d}V}{\mathrm{d}t}\left(\frac{t - l_-}{l_+ - t}\right)^\upsilon \frac{\mathrm{d}t}{t - l_+} = 0 \tag{47}$$

Substitution of (45) into (12) in view of (16a) and use of Cauchy theory (BGB) gives

$$\int_L \frac{dV}{dt}\left(\frac{t-l_-}{l_+-t}\right)^{\upsilon} dt = -\frac{A_\varepsilon D_\Omega}{c_{44} R_\varepsilon} F \tag{48}$$

Eqs. (47) and (48) provide the auxiliary formulas necessary to determine $(l, l_\pm)$. To illustrate this and also the determination of whether or not unilateral constraint (13) and (15) can be satisfied, we consider the generic parabolic die

$$V = V_0 + V_1\xi + \tfrac{1}{2}V_2\xi^2 \tag{49}$$

Here $(V_0, V_1, V_2)$ are real constants with dimensions of length. Substitution into (47) and (48) and use of Cauchy theory (BGB) gives the formulas

$$V_1 + V_2(l_+ + \upsilon l) = 0, \; l^2 + \frac{4\Omega A_\varepsilon}{\pi\upsilon(1+\upsilon)R_\varepsilon}\frac{F}{c_{44}V_2} = 0 \tag{50}$$

for $(l, l_+, l_- = l_+ - l)$. Use of (50) and Cauchy theory (BGB) in (45) then yields

$$\sigma = -\frac{2\sin\pi\upsilon}{\pi\upsilon(1+\upsilon)}\frac{F}{hl^2}(l_+-\xi)^{1+\upsilon}(\xi-l_-)^{-\upsilon} < 0 \quad (\xi \in L) \tag{51}$$

It is noted that (51) is not only bounded, but vanishes continuously at $\xi = l_\pm$.

It is also seen, in view of (35) and (46b), that (50) implies $V_2 < 0$ for $0 < c < c_R^\varepsilon$ but, if super-Rayleigh/subsonic sliding speeds ($c_R^\varepsilon < c < 1$) are allowed, then (50) implies $V_2 > 0$. Both cases satisfy in light of (51) the unilateral constraint (13). To examine this situation, (45) and (49) are used to obtain for the half-space surface outside the contact zone ($\eta = 0$, $\xi \notin L$) the formulas

$$u_{2,\xi} = -V_2[\upsilon l + l_+ - \xi - (l_+-\xi)^{1+\upsilon}(l_- - \xi)^{-\upsilon}] \tag{52a}$$

$$u_{2,\xi\xi} = -V_2\left[\left(\frac{l_+-\xi}{l_--\xi}\right)^{\upsilon}\left(1+\upsilon+\upsilon\frac{l_+-\xi}{l_--\xi}\right) - 1\right] \tag{52b}$$

Eq. (52a) exhibits continuity at the contact zone edges ($\xi = l_\pm$), while (52b) shows that the half-space curvature behaves at both edges as $\pm\infty$ for $V_2 < 0$ and $V_2 > 0$, respectively. Schematics for the two cases of possible surface deformation, that also satisfy (13), are given in Fig. 2. The case $V_2 > 0$ is seen to be artificial, so that the restriction (38) does more than avoid singular behavior. This result is known for the frictionless isotropic isothermal problem as well (Georgiadis and Barber, 1993).

The remaining unilateral constraint (15) gives (BGB) in view of (39), (41), (43), (45) and (49) the inequality

$$-V_2 S \leqslant h \tag{53a}$$

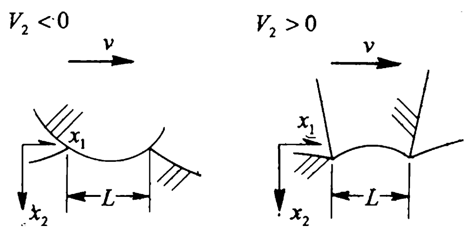


Fig. 2. Schematics of surface deformation for parabolic die.

$$S = \frac{1}{D_\Omega}\left[1 + C_L\frac{B}{A_\varepsilon} - \mu^2\frac{B}{A_\varepsilon}\left(1 + C_M\frac{B}{A_\varepsilon}\right)\right](l_+ - \xi)^{1+\upsilon}(\xi - l_-)^{-\upsilon} + \mu\frac{B}{A_\varepsilon}(l_+ - \xi - \upsilon l) \tag{53b}$$

The dimensionless quantity $S > 0$ for some values of $\xi \in L$, so that the local constraint (53a) is not automatically satisfied. Following Brock and Georgiadis (2000), a global constraint is sought: First, the roots of $\mathrm{d}S/\mathrm{d}\xi$ are examined in order to find maximum positive values of $S$. Use of the argument principle (Hille, 1959) shows that only one such root, $\xi = \xi_0$, exists for $\xi \in L$. The same approach (NAB) used for (36) gives

$$\xi_0 = \frac{l_+ + l_- x_0}{1 + x_0} \quad (\xi_0 \in L) \tag{54a}$$

$$x_0 = \frac{-1}{G_0}\left(1 + \frac{1}{\upsilon}\right) > 0, \quad \ln G_0 = -\frac{1}{\pi}\int_0^\infty \frac{\phi \mathrm{d}t}{t} \tag{54b}$$

$$\phi = \tan^{-1}\frac{2\mu\Omega\frac{B}{A_\varepsilon}}{\left[\mu^2\frac{B}{A_\varepsilon}\left(1 + C_M\frac{B}{A_\varepsilon}\right) - 1 - C_L\frac{B}{A_\varepsilon}\right][t^\upsilon + \upsilon t^\upsilon(l - t)] - \mu^2\frac{B}{A_\varepsilon}\left(1 + C_M\frac{B}{A_\varepsilon}\right)} \tag{54c}$$

Substitution of (54) into (53a,b) in light of (50) leads to the global constraint

$$-\frac{4\mu\Omega B}{\pi(1+\upsilon)R_\varepsilon}\frac{F}{c_{44}h}\frac{1}{\xi_0 - l_- - \upsilon l} \leqslant 1 \tag{55}$$

The upper bound imposed on the compressive load $F$ is more severe as the sliding speed nears its allowable maximum ($c \to c_R^\varepsilon$).

## 9. Surface thermal effects

The counterparts to (39) and (41) for the temperature change $\theta$ reduce for the contact zone ($\eta = 0, \xi \in L$) to

$$c_{44}\tilde{\alpha}\theta = \frac{\alpha}{R_\varepsilon}(C_a A_\varepsilon + C_b B)\sigma - 2\mu\frac{\alpha\Omega C_B B}{\pi R_\varepsilon}(P)\int_L \frac{\sigma \mathrm{d}t}{t - \xi} \tag{56}$$

Here the dimensionless quantities

$$DC_a = K_\Gamma(T - T_\varepsilon) + L_\Gamma B^2(A_\varepsilon^2 - A^2) \tag{57a}$$

$$DC_b = K_\Gamma(A^2 - A_\varepsilon^2) + L_\Gamma(TA_\varepsilon^2 - T_\varepsilon A^2) \tag{57b}$$

$$DC_B = M_\Gamma(T_\varepsilon - T) + N_\Gamma(A^2 - A_\varepsilon^2) \tag{57c}$$

vanish appropriately in view of (20), (24), (26) and (29) for the isothermal limit.

Substitution of (45) and (49) into (56) and use of Cauchy theory (BGB) gives

$$h\tilde{\alpha}\theta = -\frac{\alpha V_2}{D_\Omega}\left[C_a + C_b\frac{B}{A_\varepsilon} + \mu^2 C_B\left(1 + C_M\frac{B}{A_\varepsilon}\right)\right](l_+ - \xi)^{1+\upsilon}(\xi - l_-)^{-\upsilon} + \alpha V_2\mu C_B\frac{B}{A_\varepsilon}(l_+ - \xi_+ + \upsilon l) \tag{58}$$

For ($\eta = 0, \xi \notin L$) the lead term in (56) vanishes, and integration is no longer singular:

$$h\tilde{\alpha}\theta = \alpha V_2\mu C_B\frac{B}{A_\varepsilon}[l_+ - \xi + \upsilon l - (l_+ - \xi)^{1+\upsilon}(l_- - \xi)^{-\upsilon}] \tag{59}$$

is the result (BGB). Eqs. (58) and (59) show that the surface temperature change is continuous at the contact zone edges, i.e. they both give

$$\theta(l_+) = \mu \frac{\alpha V_2}{h\tilde{\alpha}} C_B \frac{B}{A_\varepsilon} \upsilon l > 0, \theta(l_-) = \left(1 + \frac{1}{\upsilon}\right)\theta(l_+) < 0 \tag{60}$$

Eq. (60) shows that the temperature change on the half-space surface vanishes (asymptotically) outside the contact zone in the absence of friction ($\mu = 0$). Because $(V_2, \upsilon) < 0$, it also shows that frictional heating occurs at the contact zone leading edge ($\xi = l_+$); the temperature actually drops at the trailing edge ($\xi = l_-$).

## 10. Sample calculations: zinc

Zinc is a category 3 hexagonal material in its isothermal state, i.e. satisfies (30c) when $(\varepsilon_1, \varepsilon_2) = 0$ (Payton, 1983). A thermoelastic study of zinc (Sharma and Sharma, 2002) yields the data

$$c_{11} = 162.8 \text{ GPa}, \quad c_{22} = 62.7 \text{ GPa}, \quad c_{12} = 50.8 \text{ GPa}, \quad c_{13} = 36.2 \text{ GPa}, \quad c_{44} = 38.5 \text{ GPa}$$

$$\rho = 7140 \text{ kg/m}^3$$

$$T_0 = 296\,^\circ\text{K}, \quad c_v = 390\,\text{J/kg}\,^\circ\text{C}$$

$$K_1 = K_2 = 124 \text{ W/m}\,^\circ\text{C}, \quad \alpha_1 = 5.818(10^6)1/^\circ\text{C}, \quad \alpha_2 = 15.35(10^6)1/^\circ\text{C}$$

These values satisfy (4a,b) and, in view of (5), (6) and (26c), give the key dimensionless parameters

$$\alpha = 1.6285, \quad \beta = 4.2301, \quad m = 2.3195, \quad m_3 = 1.9403, \quad \gamma = 2.506$$

$$\alpha_\varepsilon = 1.7203, \quad \beta_\varepsilon = 4.3042, \quad m_\varepsilon = 2.4019, \quad \gamma_\varepsilon = 2.6354$$

$$\Gamma_1 = 4.6018, \quad \Gamma_2 = 5.1181$$

and (effective) thermoelastic characteristic length

$$h = 0.019178\,\mu\text{m}$$

It is seen that the thermoelastic terms $(\alpha_\varepsilon, \beta_\varepsilon, m_\varepsilon, \gamma_\varepsilon)$ are, in keeping with the theory of linear coupled thermoelasticity (Boley and Wiener, 1985), perturbations of their isothermal counterparts $(\alpha, \beta, m, \gamma)$. The thermoelastic terms do satisfy Eq. (30c), and their use in (31a) and (36) gives the dimensionless speed parameters

$$c' = 0.9999, \quad c_R^\varepsilon = 0.8833$$

Because $c_R^\varepsilon < c'$ the restriction to sub-critical sliding means that the case for $0 < c < c'$ applies, e.g. (33) and (39) hold.

Some effects of friction on thermoelastic sliding indentation can be seen in the contact zone size $L = hl$. As an example, consider the simple parabolic profile arising from (49) when $V_1 = 0$. Then (50) produces the formula

$$\frac{L}{L^*} = 2\sqrt{\frac{A_\varepsilon \Omega}{\pi \upsilon (1 + \upsilon) R_\varepsilon}}, \quad L^* = \sqrt{\left|\frac{F}{c_{44} V_2}\right|} h \tag{61}$$

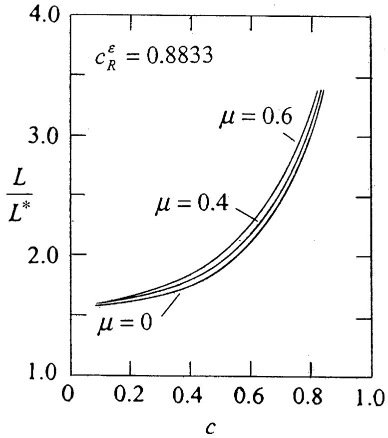


Fig. 3. Dimensionless contact zone size vs. dimensionless sliding speed.

Plots for zinc of the dimensionless ratio $L/L^*$ vs. sub-critical ($0 < c < c_R^\varepsilon = 0.8833$) $c$ are given in Fig. 3 at various values of the friction coefficient $\mu$. These show that contact zone size increases with both friction and sliding speed. The variation with speed is more pronounced.

Another quantity of interest is the contact zone average temperature change

$$\tilde{\theta} = \frac{1}{l}\int_L \theta \, \mathrm{d}\xi \tag{62}$$

Substitution of (58) into (62) and use of Cauchy theory (BGB) gives for the same ($V_1 = 0$) parabolic die the formula

$$\frac{\tilde{\theta}}{\tilde{\theta}^*} = -\frac{\alpha L^*}{LR_\varepsilon}\left[C_a A_\varepsilon + C_b B - 2\mu \frac{C_B B \Omega (1+2\upsilon)}{\pi \upsilon (1+\upsilon)} + \mu^2 C_B B\left(1 + C_M \frac{B}{A_\varepsilon}\right)\right] \tag{63a}$$

$$\tilde{\theta}^* = \frac{F}{c_{44} h \tilde{\alpha}} \tag{63b}$$

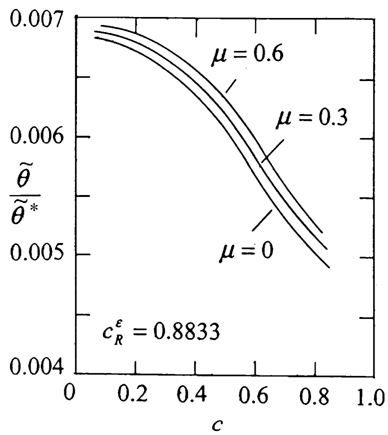


Fig. 4. Dimensionless average contact zone temperature change vs. dimensionless sliding speed.

Plots for zinc of the dimensionless ratio (63a) vs. sub-critical $c$ at various values of $\mu$ in Fig. 4 show that the average temperature change is always positive. The variation with both speed and friction is not as pronounced, however, as that displayed in Fig. 3. The more-sensitive speed variation is, moreover, an inverse one.

## 11. Comments

Robust asymptotic solutions have been obtained analytically for sliding indentation in the dynamic steady-state on a transversely isotropic thermoelastic half-space by a rigid die in the presence of friction. The analysis was two-dimensional, the die was insulated and its profile, smooth. Sliding could occur at any constant sub-critical value, and all auxiliary conditions—including two unilateral constraints—that are required for physically acceptable solutions were imposed.

The solution was examined for the case of a generic parabolic die, and equations for the contact zone size and location derived. The solution also indicated that sub-critical sliding arises for sliding speeds below the thermoelastic Rayleigh wave value. Singular behavior occurs at the Rayleigh speed, and speeds in the super-Rayleigh/subsonic range lead to an artificial result in order that the first unilateral constraint—that contact zone normal stress is non-tensile—be satisfied. This speed-related behavior is consistent with isotropic/isothermal sliding indentation studies (Georgiadis and Barber, 1993; Brock and Georgiadis, 2000; Brock, 2002).

The second unilateral constraint arises under a strict interpretation of the local application of the Coulomb model: the contact zone shear stress work-rate must be negative. It was found that the local constraint is not automatically satisfied, but that a global constraint for the total compressive force on the die can be extracted. Violation of this constraint implied that a displacement gradient magnitude approaches unity, which in turn would violate the linearity of the analysis. However, the global inequality shows that this scenario arises generally for sliding speeds near the critical subsonic (Rayleigh) value. At that speed, the solution becomes unbounded in any case.

It was found that the temperature change (asymptotically) vanishes on the half-space surface outside the contact zone in the absence of friction. With friction, the temperature at the trailing edge of the zone might actually drop. Calculations showed, however, that the average contact zone temperature always increases. This average varies directly with friction and inversely with sliding speed. Both variations were small when compared to the direct variations seen with both parameters in calculations for the contact zone size.

In general (Payton, 1983; Norris and Achenbach, 1984) solution forms for dynamic anisotropic elasticity are more complicated than their isotropic counterparts. Following BGH, however, certain factoring procedures were used in this article to simplify these forms. As noted in the former article, similar factorizations could in fact be used to advantage in the isothermal case. This study also required the extraction of certain roots of irrational functions, and the work of NAB provided an approach that produced expressions analytical to within a single quadrature.

The solution forms obtained here were, in the full field, sensitive to categories of dimensionless isothermal elastic constants. The categorization followed the three-element system used for isothermal transverse isotropy by Payton (1983). It was found here that (a) the three categories coalesced into two in so far as distinguishing solution form is concerned and (b) even these two categories lost their distinctiveness on the half-space surface itself. It should be noted that the isothermal and thermoelastic categories might not coincide for a given material. Although thermoelastic coupling may only perturb the isothermal material constants, e.g. zinc, a material that exists near the edge of one category isothermally may move into the adjacent category thermoelastically.

It should also be noted that the present analysis ignored the possibility of contact zone adhesion, i.e. when tangential speeds of surface points equal the sliding speed. The present results are now being applied to dynamic fracture studies that include this possibility, and to purely transient analyses of contact. It is hoped, however, that the present results stand on their own in shedding some light on the rapid sliding indentation of anisotropic thermoelastic solids.

## References

Blau, P.J., 1996. Friction Science and Technology. Marcel Dekker, New York.
Boley, B.A., Wiener, J.H., 1985. Theory of Thermal Stresses. Krieger, Malabar, FL.
Brock, L.M., 1981. Sliding and indentation by a rigid half-wedge with friction and displacement coupling effects. International Journal of Engineering Science 19, 33–40.
Brock, L.M., 1998. Analytic results for roots of two irrational functions in elastic wave propagation. Journal of the Australian Mathematical Society Series B 40, 72–79.
Brock, L.M., 1999. Rapid sliding indentation with friction of a pre-stressed thermoelastic material. Journal of Elasticity 53, 161–188.
Brock, L.M., 2002. Exact analysis of dynamic sliding indentation at any constant speed on an orthotropic or transversely isotropic half-space. ASME Journal of Applied Mechanics 69, 340–345.
Brock, L.M., Georgiadis, H.G., 2000. Sliding contact with friction of a thermoelastic solid at subsonic, transonic and supersonic speeds. Journal of Thermal Stresses 23, 629–656.
Brock, L.M., Georgiadis, H.G., Hanson, M.T., 2001. Rapid indentation of transversely isotropic or orthotropic half-spaces. ASME Journal of Applied Mechanics 68, 490–495.
Carrier, G.F., Pearson, C.E., 1988. Partial Differential Equations. Academic Press, New York.
Craggs, J.W., Roberts, A.M., 1967. On the motion of a heavy cylinder over the surface of an elastic half-space. ASME Journal of Applied Mechanics 24, 207–209.
Erdogan, F., 1976. Mixed boundary value problems in mechanics. In: Nemat-Nasser, S. (Ed.), Mechanics Today, Vol. 4. Pergamon, New York.
Georgiadis, H.G., Barber, J.R., 1993. On the super-Rayleigh/subseismic elastodynamic indentation problem. Journal of Elasticity 31, 141–161.
Hille, E., 1959. Analytic Function Theory, vol. I. Blaisdell, Waltham, MA.
Muskhelishvili, N.I., 1975. Some Basic Problems of the Mathematical Theory of Elasticity. Noordhoff, Leyden.
Norris, A.N., Achenbach, J.D., 1984. Elastic wave diffraction by a semi-infinite crack in a transversely isotropic material. Quarterly Journal of Mechanics and Applied Mathematics 37, 565–580.
Payton, R.G., 1983. Elastic Wave Propagation in Transversely Isotropic Media. Martinus Nijhof, The Hague.
Peirce, B.O., Foster, R.M., 1956. A Short Table of Integrals. Blaisdell, Waltham, MA.
Sharma, J.N., Sharma, P.K., 2002. Free vibration of homogeneous transversely isotropic thermoelastic cylindrical panel. Journal of Thermal Stresses 25, 169–182.
van der Pol, B., Bremmer, H., 1950. Operational Calculus on the Two-Sided Laplace Integral. Cambridge University Press, London.